LAWRENCE
LIVERMORE
NATIONAL
LABORATORY

UCRL-PROC-201756

Jet propagation through energetic materials

Philip Pincosy, Peter Poulsen

January 9, 2004

International Symposium on Ballistics
Adelaide, Australia
April 19, 2004 through April 23, 2004

Disclaimer

JET PROPAGATION THROUGH ENERGETIC MATERIALS

Dr. Philip Pincosy*, Dr. Peter Poulsen
Lawrence Livermore National Laboratory
P.O. Box 808 L-099
Livermore, CA 94551

In applications where jets propagate through energetic materials, they have been observed to become sufficiently perturbed to reduce their ability to effectively penetrate subsequent material. Analytical calculations of the jet Bernoulli flow provides an estimate of the onset and extent of such perturbations. Although two-dimensional calculations show the back-flow interaction pressure pulses, the symmetry dictates that the flow remains axial. In three dimensions the same pressure impulses can be asymmetrical if the jet is asymmetrical.
The 3D calculations thus show parts of the jet having a significant component of radial velocity. On the average the downstream effects of this radial flow can be estimated and calculated by a 2D code by applying a symmetrical radial component to the jet at the appropriate position as the jet propagates through the energetic material. We have calculated the 3D propagation of a radio graphed TOW2 jet with measured variations in straightness and diameter. The resultant three-dimensional perturbations on the jet result in radial flow, which eventually tears apart the coherent jet flow. This calculated jet is compared with jet radiographs after passage through the energetic material for various material thickness and plate thicknesses. We noted that confinement due to a bounding metal plate on the energetic material extends the pressure duration and extent of the perturbation.

INTRODUCTION

The propagation of jets through high explosive (HE) materials [I, 21 becomes perturbed by varying degrees depending on a number of parameters. These perturbations affect the subsequent capability of the jet to penetrate further material layers in the path. The Bernoulli flow of the jet stagnates and reverses its relative direction while eroding into the material. The perturbations are produced as the back-flowing jet material is pushed down onto the in-flowing jet by the HE pressure and radial momentum is exchanged. In the axis-symmetry of 2D calculations the momentum exchange by the impingement of the back-flowing ribbon on the in-flowing jet symmetrically compresses the incoming jet material. The pressure pulses propagate up and down the jet. In 3D the breakup of the real jet apparently results from the small asymmetry of jet flow produced in its formation. A close look at a radiograph of a developed jet shows diameter variations and straightness variation from the tip to the tail. The supposition is that these variations will cause asymmetry in the back-flow and thus asymmetric momentum exchange with the in-flowing jet. We calculate in 3D the jet flow through HE, thick enough to create such perturbations. We will discuss the

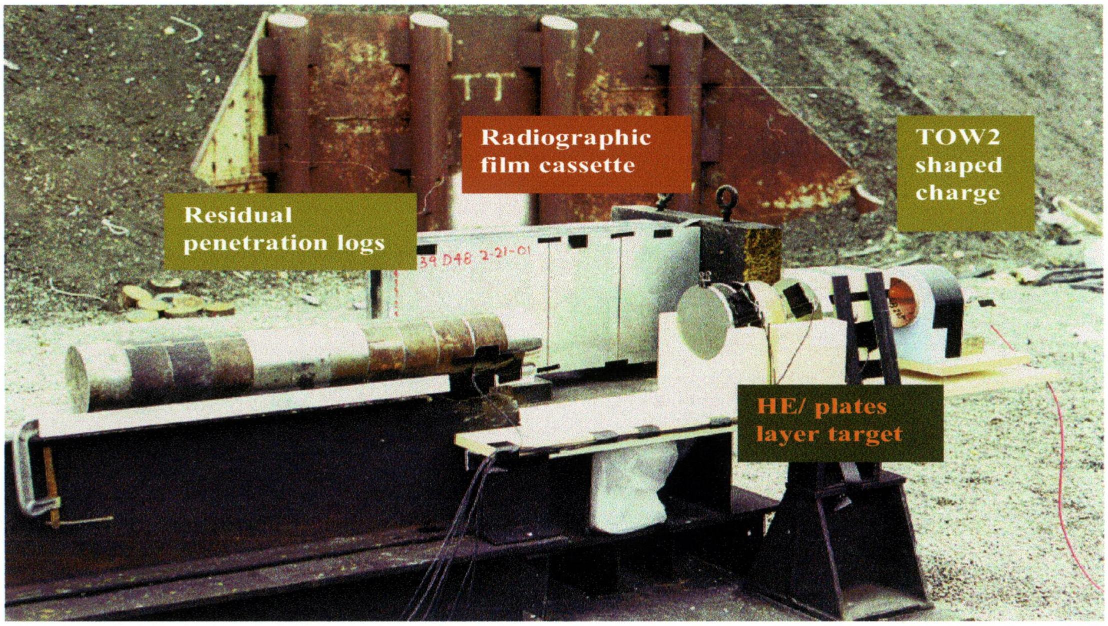

FIGURE 1. Typical experimental jet test setup.

required calculation resolution and the limitations of material models to fully calculate the flow response once the perturbations are seeded. As the HE pressure falls the back-flow interactions should eventually be released. Experimental results show [2] that confinement of the HE by a back plate causes jet flow perturbations over a longer part of the jet.

We will show that the 3D calculations of an input jet with axial variations results in an angular divergence of the jet flow after leaving the confined region in the HE. This is compared with the experiments. As the jet propagates away from the confined region the continued radial spread will reduce the penetration capability of the jet. A series of tests [2] using the TOW2A copper jet having a tip velocity of 9.5 km/s were done to measure the development of perturbations on the jet after having passed through HE. The typical experimental setup is shown in Fig 1 with the main diagnostic being a radiograph of the jet in flight. The principal components of the test are labeled on the photograph.

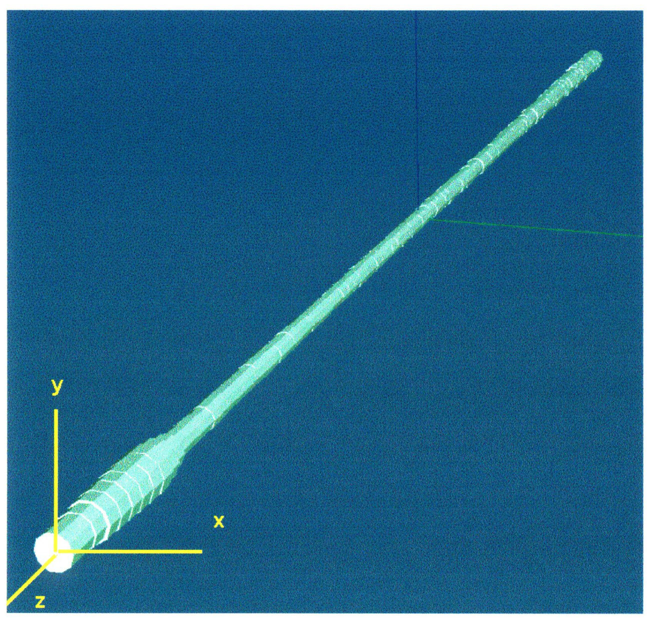

FIGURE 2. TOW2. jet rendered as a series of cylinders with radii matching the radiograph.

CALCULATION PROCESS

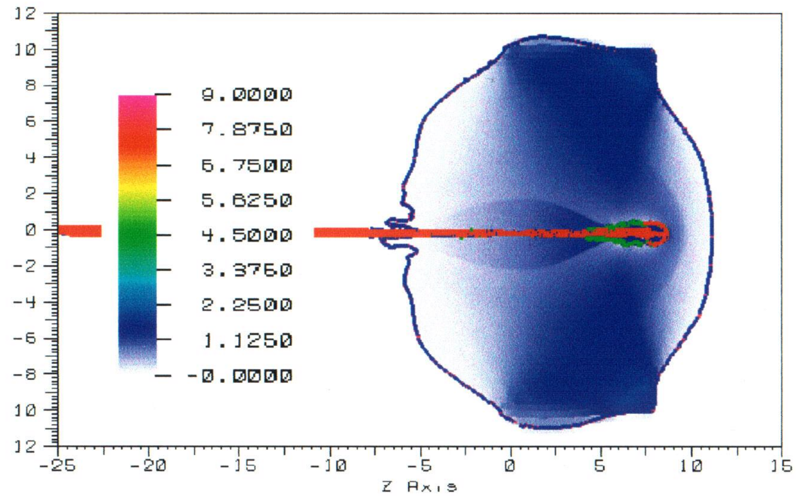

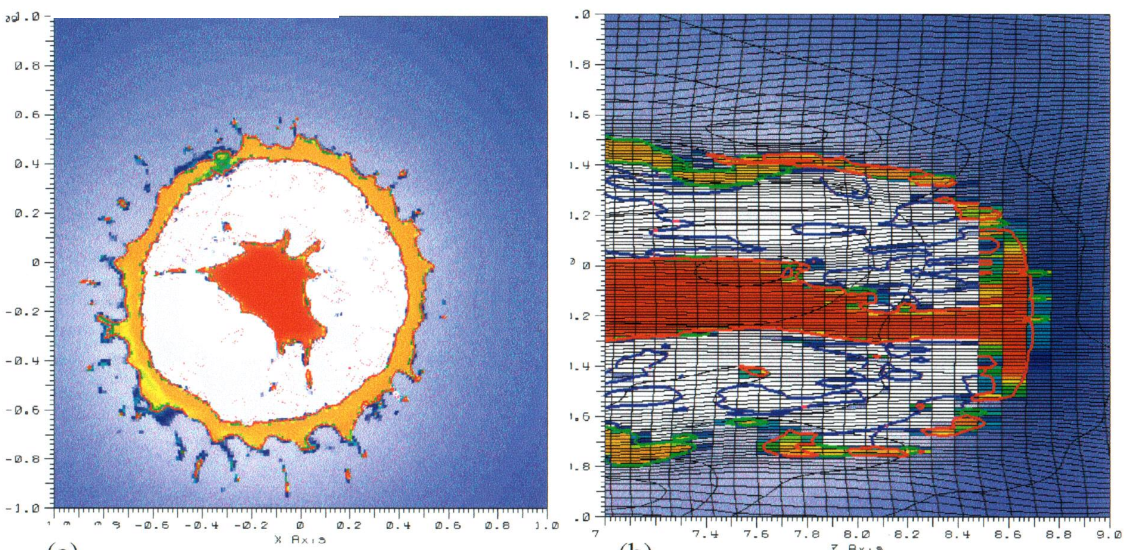

(a) (b)

In order to provide a realistic input jet for the 3D calculations, we took a radiograph of the TOW2 jet stretched to 4.8 charge diameters. We accurately measured the edges defining the jet diameter as a function of the length. The average straight line through the center points defined a jet axis. The 3D jet was input as a series of cylinders (Fig 2) with centers varied according to the measured edges. The displacement of the cylinder centerlines were chosen to be the same in the two transverse directions for lack of knowledge about the real variations in the non-radio graphic direction. The maximum transverse displacement (about 1.5 mm) off the average centerline was as much as half the local diameter and this offset slowly increased from the tip to the tail.

In performing the calculations with ALE3D we set up the region of space in a cylindrical geometry with 10 cm radius cylinder and reduced conductivity central region having a highly resolved uniform mesh out to1.25 cm and graded to large zones near the outer radius. The highest radial calculated resolution in the central region including the jet and associated backflow (Fig 3b) was slightly larger than 0.1 mm zone size depending on the material. ALE3D is a Lagrange/Eulerian code with mesh density weighting associated with material. The jet copper material flow is weighted three to four times the weighting in the HE. The resolution in the axial direction was about 1 mm. The HE and backing plates were included, as used in experiments. The jet flow several 10's of microseconds after leaving the HE and/or backing plate was compared to the radiograph of the experiment.

REAL JET EFFECTS

Two experiments are compared with 3D calculations. The first is the TOW2 jet erosion and propagation through 8 cm of CompB HE and the second experiment is with the same HE, backed up by a steel plate 1.25 cm thick. The TOW2 jets are radio-graphed after exiting the HE or the plate. From previous experiments it has been observed [1] that the TOW2 jet begins to be perturbed upon eroding through more than 4 to *5* cm of CompB HE.

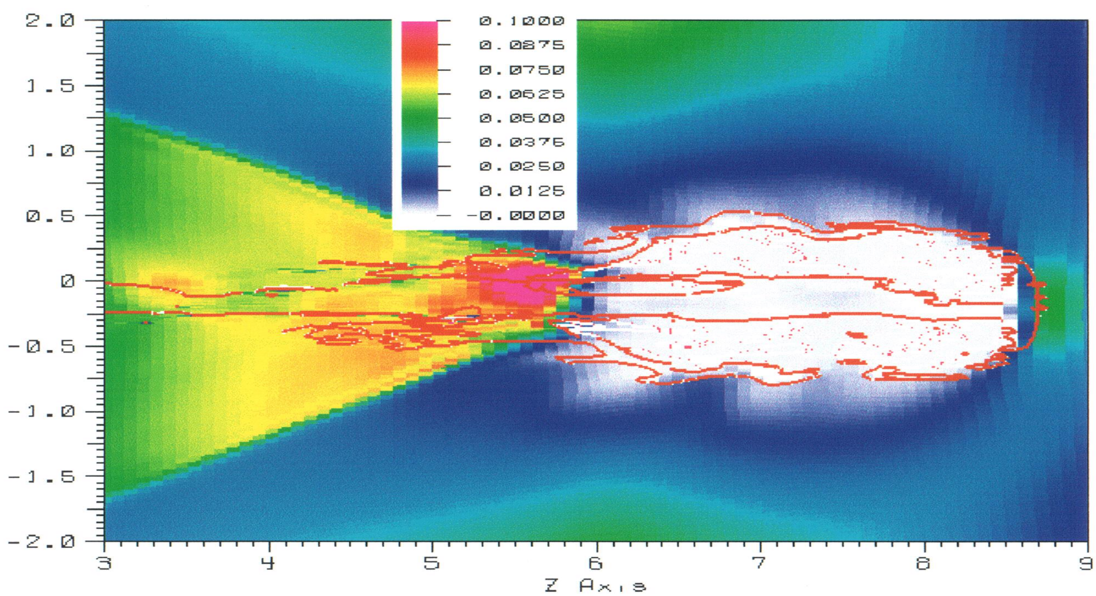

Figure 4. Asymmetric pressure distribution on the jet flow due to back-flow interaction. Pressure range from 0 to 100 kB. Red outline represents the boundary of the copper jet material. Calculation time at 15 us.

In Fig 3 we show the calculated TOW2 copper jet at 15 us of calculation time -about 14 us after entering the HE. The perturbations have been developing for a few microseconds and the pressure around the back-flow material has dropped to about 10 kB. The average density of the calculated back-flow (Fig 3a) is lower than the core jet density because the resolution is barely adequate and there are many mixed zones giving a lower average density indicated by the color plot. The calculation of the copper jet includes strength for the copper and other plates. The separation of stretching materials (Fig 3b) is computational due to resolution or set limits on the minimum density for validity of the equation of state. Once the material is stretched to the minimum negative pressure or yield stress, it remains at this value or is set to zero. Once the jet is in free space we set the minimum stress to zero. This permits a free expansion of the material according to the radial momentum induced during the jet back-flow interaction. Note the back-flow material (Fig 3 a & b) at about 5 mm with average thickness of about 0.4 mm. Outside this back-flow region (Fig 4) the pressure in the HE is about 10 kB and zero inside the back-flow. This external pressure is still sufficient to push the back-flow down onto the in-flowing jet. Note the high-pressure (> 100 kB) interaction at the z= 5.5 cm back-flow impingement location. A shock cone produces a pressure of 60 kB. The back-flowing material bounces off the interaction point and is pushed back down to interact again at 5.0 cm (17 us in calculation time). The in-flowing jet material at the interaction point shown in Fig 4 has then propagated to 7 cm (TOW2 jet material velocity is 9 mm/us at this location). Fig 3b shows the back-flow material interacting with the in-flowing jet material.

We also calculate the jet erosion dynamics when the HE is backed up with a steel plate. The plate adds confinement to the expanding HE and keeps the pressure elevated during the time of jet erosion through the plate. During the erosion through the steel plate the back-flowing copper is strongly pushed onto the in-flowing jet enhancing the perturbations as shown in Fig 5. The surrounding pressure during this time is 20 to 30 kB. The erosion rate

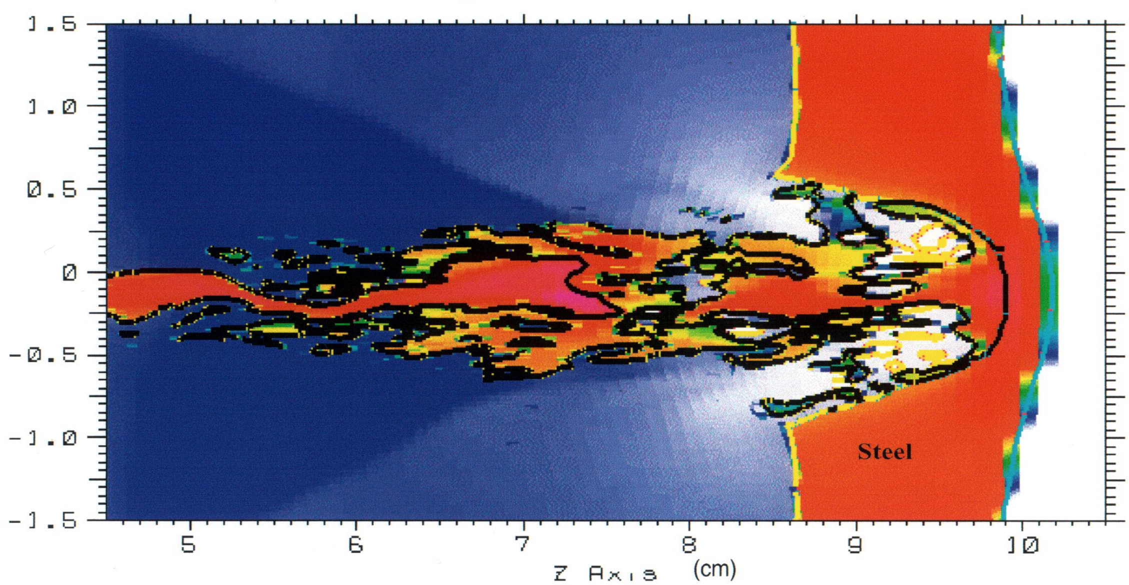

into the steel relative to the erosion rate into HE is reduced by 25 percent, so the back-flowing copper produced during the erosion in the HE is piling up with the faster back-flowing jet copper produced in momentum balance with the steel. The resultant mixed and perturbed jet material is as shown in Fig *5*.

Comparison with experimental measurements

The calculated hydrodynamic response of jet erosion through HE provides a dramatic illustration of the development of 3D perturbations on the normal axis-symmetric flow of jet propagation. We have suggested limitations with the calculations as performed. The calculation may obtain the right quantity of radial momentum provided the input jet has a representative variation of the actual jet in an experiment. In Fig 6 we show a comparison between calculation and an experiment with only a small amount of perturbation propagation. The experiments [2] established the HE thickness between 4 and 5 cm as the threshold for the onset of perturbations. Our calculation and analytic calculations [3] showed back-flow impingement at 4 cm in good agreement. The only measurable time available to compare calculation with experiment is a later time record of jet flow as shown in Fig 7. The earliest radiograph available was at 54 us. The calculation takes many weeks so we present an earlier time result. The top calculation shows more dispersed material back to the

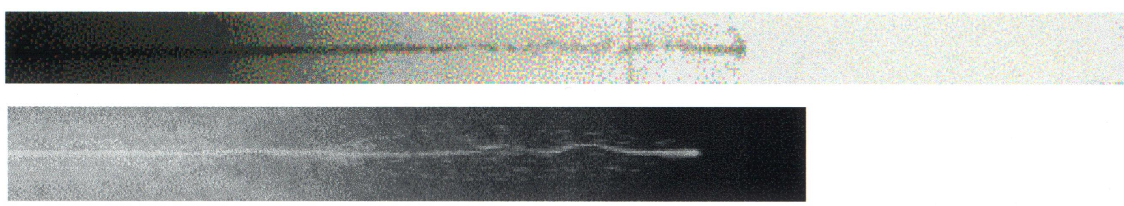

FIGURE 6. Comparison of calculated and experimental TOW2 jet through thin HE.
Upper: Radiograph of TOW2 jet after passing through 5.1 cm of HE
Lower: Calculated 3D simulation radiograph of TOW2 jet after passing through 5.1 cm HE

point of latest perturbations at 14 cm. If this view was done as a simulated radiograph it may have looked more similar to the radiograph since the radio graph measures integrated line density. We would not expect the structure to be comparable in detail since the real input is certainly different. It is clear that the added steel backing plate contributes to more radial momentum and a longer duration (compare the bottom radio-graph to the top). The calculation for the case with the steel backing plate is 2 cm shorter because of the added time to penetrate the plate. The perturbations continue back to 11 cm compared to 14 for no plate (compare the bottom calculation to the top). Also in the radiograph we see the same qualitative result. The particles of copper calculated in the bottom view are blue and are

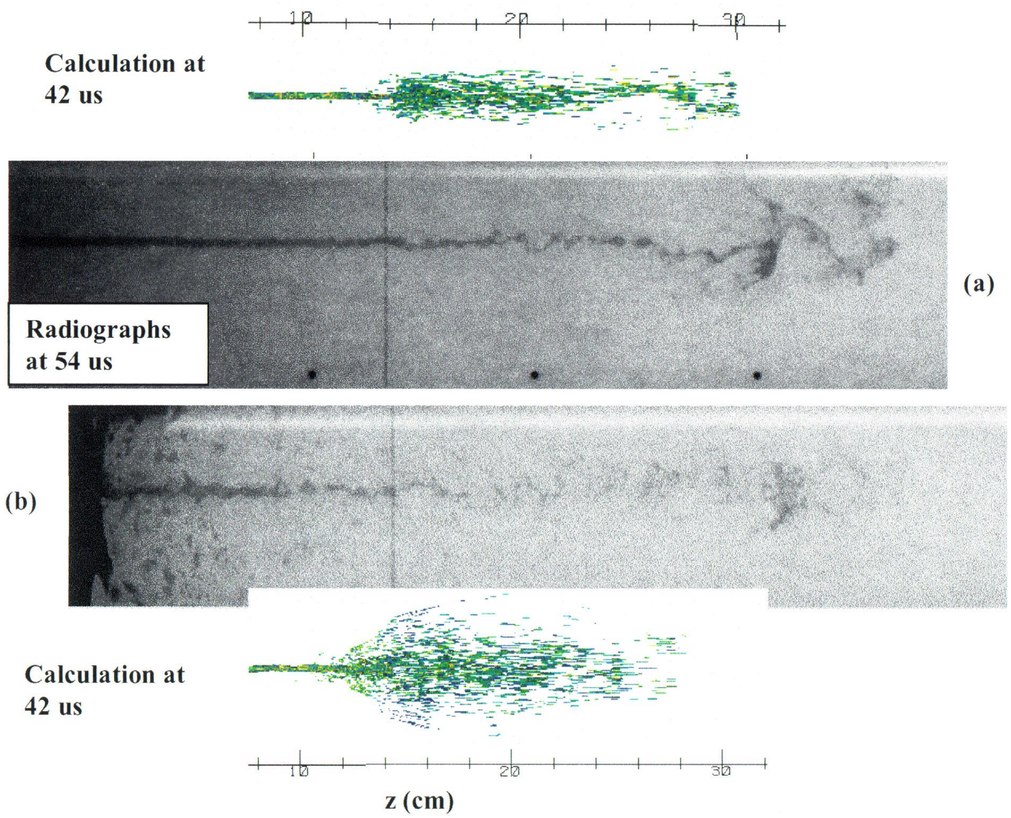

mixed material clumps of zones with lower average density. It may be that a radiograph would not have sufficient line density to register these blue pieces in the film. These clumps represent numerically separated regions due to material tension and shear.

The development of shaped charge penetration capability has been studied through 3D calculations. The calculations clearly show how radial jet flow is developed through back-flow interaction with in-flowing jet. It is clearly the small variations in the diameter and flow center relative to the back-flow that give rise to non-symmetrical pressure variations and thus radial momentum growth. HE thickness, backing plate thickness or mass, contributes to confinement duration of the HE in terms of pressure decay. The penetration capability of the perturbed portion of the jet depends upon the above parameters and the flow distance between perturbation location and the penetration location. This onset of perturbations have been analytically modeled as well as calculated both by 2D and 3D hydro. The 3D calculation represents perturbation growth and gives a qualitative match to the experimental data, but resolution, although good limits how material flow can separate. Clearly a better representation should include material fracture and is available for future effort.

Acknowledgement

This work was performed under the auspices of the U. S. Department of Energy by the University of California Lawrence Livermore National Laboratory under contract No. W-7405-ENG-48

References

1. P. Poulsen, "Jet Penetration of High Explosive", 18th International Symposium on Ballistics, 1999.
2. P. Poulsen, "Jet Perturbation by HE Target", 19th International Symposium on Ballistics, 2001
3. R. P. Godwin, and E. J. Chapyak, "Apparent Target Strength in Long-rod Penetration", Int J. Impact Eng. 21, p77, (1 998).